Effect of water pressure on time-dependent permeability characteristics of sand conditioned with foam and bentonite slurry

Shuying Wang[1], Fanlin Ling[2,*], Qinxin Hu[3], Tongming Qu[4], Junlong Shang[2]

1 College of Civil and Transportation Engineering, Shenzhen University, Shenzhen 518060, China.

2 School of Mechanical, Aerospace and Civil Engineering, The University of Manchester, Manchester M13 9PL, United Kingdom.

3 Department of Civil and Environmental Engineering, University of Strathclyde, Glasgow G1 1XJ, United Kingdom.

4 Department of Civil and Environmental Engineering, Hong Kong University of Science and Technology, Hong Kong, China.

Shuying Wang. Email: swang24@szu.edu.cn

Fanlin Ling. Email: fanlin.ling@postgrad.manchester.ac.uk

Qinxin Hu. Email: qinxin.hu@strath.ac.uk

Tongming Qu. Email: tongmingqu@ust.hk

Junlong Shang. Email: junlong.shang@manchester.ac.uk

**** corresponding author: Fanlin Ling***

Abstract: During earth pressure balance (EPB) shield tunnelling in water-rich sandy ground, both foam and other conditioning agents, such as bentonite slurry, are injected to prevent water spewing. Permeability tests were conducted to investigate how water pressure affects the permeability of sand conditioned with foam and bentonite slurry. Experimental results demonstrate that increasing water pressure at the top and bottom of the specimen extends the initial stable period of the permeability coefficient, significantly slowing down its growth rate during the fast growth period. Soil grain migration was observed in specimens exposed to sufficiently high water pressure. During the slow growth period, the permeability coefficient decreased as water pressure increased, and this decrease rate correspondingly decreased. Under a consistent hydraulic gradient, increased water pressure led to enhanced stability of foam bubbles and extended the time-dependent curves for the permeability coefficient. Furthermore, the relationship between chamber pressure dissipation and foam stability

was discussed during the standstill period of shield machines. To prevent water spewing, it is recommended to use the permeability coefficient of the muck at the outlet of the screw conveyor with the lowest water pressure as the evaluation index during permeability testing.

Keywords: sand conditioning, foam, bentonite slurry, permeability, water pressure

1. Introduction

When earth pressure balance (EPB) shields pass through water-rich sandy ground, water spewing can easily occur, leading to challenges in controlling excavation chamber pressure and ground settlement (Peila et al. 2007; Peila et al. 2009; Budach and Thewes 2015; Feng et al. 2023). Injecting conditioning agents into the excavation chamber and screw conveyor is necessary to condition soil, ensuring that the resulting muck has suitable workability and a low permeability coefficient (Mori et al. 2017; Wang et al. 2021a; Chen et al. 2022). Generally, it is recommended that the permeability coefficient of muck be less than 10^{-5} m/s and maintained for at least 90 min (Wilms 1995; Quebaud et al. 1998; Peila 2014).

Foam, a major conditioning agent, finds wide application in sandy ground (Langmaack and Lee 2016). Great efforts have been devoted to investigating the permeability characteristics of foam-conditioned sands. Borio and Peila (2010) conducted constant head permeability tests to study the effects of foam injection ratio (*FIR*, which is defined as the ratio of the volume of foam to that of a soil specimen) and foam expansion ratio (*FER*, which is defined as the ratio of the volume of foam to that of foam solution) on the permeability of foam-conditioned sand and found that the permeability coefficient of conditioned sand decreased with an increase in *FIR* and a decrease in

FER. Quebaud et al. (1998) found that when *FIR* increased to a certain value, adding extra foam would no longer have an impact on the permeability of conditioned sand, which would tend to be stable. Meanwhile, it was pointed out that the foaming agent containing polymer had a more significant reduction effect on the permeability of the sand. Bezuijen et al. (1999) proposed that adding a certain amount of foam to sand can significantly reduce its permeability, and the level of reduction was related to the fact that foam bubbles fill in the soil pores. Huang et al. (2019) conducted permeability tests on foam-conditioned soil and found that effective grain size (d_{10}) was an important factor affecting the permeability characteristics of the conditioned soil. Further, adding fine particles to a certain extent could reduce the permeability of foam-conditioned soil. Wang et al. (2020a) conducted permeability tests on foam-conditioned sand with different workability states, and found that the permeability coefficient with suitable workability could better meet the requirements of maintaining at least 90 min with a value of lower than 10^{-5} m/s. Considering the effect of hydraulic gradient on the permeability of foam-conditioned sand, Hu et al. (2020) pointed out that the permeability coefficient of foam-conditioned sand grew rapidly with an increase in hydraulic gradient, the suitable conditioning parameters should be in the direction of a low water content (w) and high *FIR* for low permeability. They also emphasized that only using foam to condition sandy soil under a high hydraulic gradient cannot meet the requirements of low permeability. Bezuijen and Dias (2017) found that when an EPB shield stays at a standstill for a long time, foam dissipation in the excavation chamber and screw conveyor would lead to pressure fluctuation. In the process of restarting shield tunnelling, not only the risk of water spewing but also the instability of the excavation face may occur.

Other agents such as bentonite could be considered for combined conditioning. Bentonite is commonly used to reduce sand permeability (Chapuis 1990; Sivapullaiah et al. 2000; Komine, 2010; Xu and Bezuijen 2019) and foamed concrete (Xie et al. 2018). Combining foam with bentonite slurry is also a prevalent method to prevent spewing under high water pressure in the field. Jancsecz et al. (1999) pointed out that using bentonite slurry to replace part of foam for combined conditioning could reduce costs. However, there are still research gaps regarding the permeability characteristics of sand conditioned with foam and bentonite slurry under high water pressure. A deeper understanding of the mechanism of combined conditioning will aid in decision-making regarding conditioning parameters for shield tunnelling in sandy ground by mitigating water spewing.

This study investigates the influence of water pressure on time-dependent permeability characteristics of sand conditioned with foam and bentonite slurry. A series of permeability tests were conducted on foam-bentonite slurry-conditioned sand, with variations in water pressure applied at both the top and bottom of the specimen. Detailed analysis of the permeability characteristics of conditioned sand under high water pressure was carried out, shedding light on the conditioning mechanism involving the combination of foam and bentonite slurry. Finally, the significance and practical applicability of conducting permeability tests on sand conditioned with foam and bentonite slurry under high water pressure in field applications were discussed.

2. Background

EPB shields are occasionally employed in tunnel projects with substantial overburden or when

passing under rivers due to their relatively lower construction and operational costs. For instance, the Túnel Emisor Oriente (TEO) project in Mexico traverses a composite ground consisting of hard rock and soft soil, including clay, sedimentary rock, basalt, and volcanic rock. The tunnel reaches a maximum burial depth exceeding 150 m, with the highest water pressure reaching 0.75 MPa (Rangel et al. 2012). Another example is the Longquan water tunnel in the Dianzhong Water Diversion Project of China, which is also being constructed with an EPB shield. In this case, the maximum burial depth is 75 m, and the highest water pressure reaches over 0.50 MPa. The hydraulic gradient between the cutterhead and discharge gate during EPB shield tunnelling ranges from 2 to 5, sometimes up to 10.l (Hu et al. 2020).

Hu et al. (2020) and Ling et al. (2022) investigated the permeability characteristics of foam-conditioned sand and foam-bentonite slurry-conditioned sand under high hydraulic gradients by adjusting the water head in the water inlet of the specimen to achieve the predefined initial hydraulic gradient. However, it's important to note that the water pressure in their studies was not sufficiently high to determine the direct effect of water pressure on the permeability characteristics of conditioned sand under the same hydraulic gradient. In reality, water pressure does indeed influence the stability of foam bubbles. These foam bubbles, present in the conditioned soil, occupy the pores between soil particles and form water-blocking structures, crucial for reducing the cross-sectional area during the seepage process. The stability of foam bubbles indirectly affects the permeability of the conditioned soil. Two primary factors influencing their stability are liquid film drainage and air exchange (Kaptay 2006; Pitois et al. 2009). Liquid film drainage involves the spontaneous flow of liquid from the film between foam bubbles to the plateau border due to pressure differences and

gravity, gradually thinning the liquid film and leading to the dissipation of foam bubbles. Air exchange phenomena include two mechanisms: coalescence and coarsening. Coalescence occurs when thin films between adjacent foam bubbles break, leading to the formation of a single large bubble. Coarsening is defined as the evolution of air diffusing from smaller bubbles to larger ones due to a pressure difference. Coarsening primarily occurs between bubbles of different sizes. Air diffuses through the liquid film from smaller bubbles to larger bubbles because of a pressure difference. Air pressure is higher in smaller bubbles. As a result, smaller bubbles dissipate, while larger ones expand and tend to merge.

Wu et al. (2020) observed a significant enhancement in foam stability within conditioned sand upon the application of pressure. This improvement manifested as a slowdown in the coarsening process, allowing foam bubbles to effectively trap themselves between sand particles. Furthermore, Bezuijen and Schaminée (2001) and Peila et al. (2007) used a self-designed screw conveyor model to conduct muck discharging tests. Their findings demonstrated that pressure dissipated linearly along the screw conveyor. Given these observations, it becomes imperative to investigate the influence of water pressure on the permeability characteristics of conditioned sand. Such an investigation is vital for effectively preventing water spewing from the screw conveyor during earth pressure balance (EPB) shield tunnelling in sandy ground, as well as during the restarting process.

3. Experimental methods

3.1. Experimental materials

The sand used in the tests was collected from the Xiangjiang River, Changsha, China. The grain

gradation of the sand was the same as that used by Hu et al. (2020) and Ling et al. (2022). Figure 1 shows the grain size distribution of the test soil. The fine particles (<0.075 mm in diameter) only comprised 0.08% of the specimen, and the sand (0.075-4.75 mm in diameter) and gravel (4.75-75 mm in diameter) particles comprised 67.87% and 32.05% of the soil, respectively. The uniformity coefficient (C_u) and the curvature coefficient (C_c) were 9.85 and 0.39, respectively. According to ASTM D2487-17 (ASTM, 2017), the soil is classified as a poorly graded sand (SP).

Table 1 lists the main chemical composition of the foam agent used in the tests. Sodium dodecyl sulphate and dodecyl ammonium chloride are foaming agents, silicone oil is a foam stabilizer. The foaming generation system, as shown in Fig. 2, met the requirements of EFNARC (2015). It allowed for full mixing of foaming solution and air in the foam generator, and the generated foam was collected. The weight concentration of the foaming solution was 3%, *FER* was 10, and the half-life duration of the generated foam was about 6 min which met the requirements of recommended *FER* in 5-30, and half-life duration above 5 min (Milligan, 2000).

Powdered sodium bentonite was tested by X-ray diffraction (XRD), and its minerals are shown in Table 2. Na-montmorillonite accounts for the highest proportion, up to 48.8%. Suitable slurry viscosity is significant for soil conditioning. On one hand, a bentonite slurry with excessively high viscosity has poor pumpability, which may cause conditioning pipeline blockage. On the other hand, a bentonite slurry with low viscosity cannot condition the hydro-mechanical property of sands properly (Kenney et al. 1992; Ma et al. 2021; Ling et al. 2024). It is recommended to use a Marsh funnel to determine slurry viscosity (API, 2003; Peila et al. 2011; Budach, 2012; Xu and Bezuijen 2018). The weight concentration of sodium bentonite slurry used in this study was 7%, and the

corresponding Marsh funnel viscosity was 45 s after a fermentation time of 18 h.

3.2. Experimental equipment and approaches

As shown in Fig. 3(a), a large-scale permeameter was developed for constant head permeability tests, which met the requirements of ASTM D2434-19 (ASTM, 2019). The permeameter was 30 cm in diameter and 75 cm in height. Two digital pressure gauges were connected to the top and bottom of the permeameter to record the water pressure. The pressure adjustment range of the permeameter was 0-0.5 MPa. In addition to the requirement of permeability, the shield muck in the sandy ground should also have suitable workability for smooth discharging by a screw conveyor. This study focuses on the investigation of permeability characteristics of conditioned sand with suitable workability. According to the results of the slump tests by Ling et al. (2022), the conditioning parameters of w=10%, FIR=10% and BIR (Bentonite slurry injection ratio) =5% were selected for carrying out permeability tests, and the conditioned sand has suitable workability in slump test, as shown in Fig. 3(b). The slump value was 18.0 cm which was in the ideal slump range of 15-20 cm (Vinai et al. 2008; Wang et al. 2020a), and there was no water and foam bleeding.

The hydraulic gradients between the cutterhead and discharge gate during EPB shield or EPB pipe-jacking tunnelling range from 2 to 5 generally, and sometimes up to 10 (Hu et al. 2020; Wang et al. 2022). So, some cases under high hydraulic gradients were chosen to test in this study. Table 3 lists specific conditions of the permeability tests. Top pressure and bottom pressure are the main variables, and the hydraulic gradient also changes accordingly.

The permeability tests were carried out according to ASTM D2434-19 (ASTM, 2019). The specific test steps for each test were as follows:

(1) The sand was mixed with a predetermined water content in a mixer for 1 min and left there to ensure that the sand specimen fully absorbed the water. Then, the bentonite slurry (pre-stirred for 5 min before use) was mixed with sand for 1 min. Subsequently, the foam was added and stirred together for another 1 min to prepare the conditioned sand.

(2) A piece of filter paper was placed on the bottom of the permeameter, and then the foam-bentonite slurry-conditioned sand was filled layer by layer into the permeameter. To prevent the possible influence of soil specimen falling from a certain height, each layer was poured gently onto the surface of the previous layer. The total height of the specimen was approximately 60 cm.

(3) The top plate of the permeameter was assembled after a piece of filter paper was placed on the top of the specimen. Then, tap water was slowly supplied to the top of the specimen. Meanwhile, the valve at the top plate was opened to release air above the specimen.

(4) After the permeameter was full of water, the valve at the top plate was closed, and one-dimensional permeation downward along the axis of the permeameter was conducted. The required water pressure was provided by changing the height of the inlet and outlet water tanks. The whole process of specimen preparation for each permeability test was conducted in approximately 25 min.

(5) The height of the specimen l (m) which changed due to foam dissipation and specimen compression) at different times during permeability tests, the volume of the seepage quantity Q (m^3), the water pressure P_t (MPa) at the top gauge and the water pressure P_b (MPa) at the bottom gauge (see Fig. 3(a)) in each short interval Δt were recorded. Considering the possibility of a long-time standstill of EPB shield, the test was carried out for a long time to fully capture the whole process of the time-dependent permeability coefficient. When the permeability coefficient increased

slowly or remained constant with time, the permeability test was halted. In the permeability test, due to the slow flow rate of water, and the assumption that the specimen is homogenous at every short measurement interval, the permeability coefficient k at different times can be calculated by using Darcy's law (Psomas 2001; Budach and Thewes 2015; Wang et al. 2020b; Wei et al. 2020).

4. Experimental Results

4.1. Permeability characteristics of foam-bentonite slurry-conditioned sand

Figure 4 illustrates the time-dependent curves of the permeability coefficient (k) of foam-bentonite slurry-conditioned sand. The permeability coefficient curves for a majority of specimens exhibit three main periods, including an initial stable period, a fast growth period and a slow growth period, similar to those observed in foam-conditioned soil (Huang et al. 2019; Wang et al. 2020b). During the initial stable period, the permeability coefficient remains low. Subsequently, as foam bubbles gradually dissipate, more permeability channels form in the conditioned sand, leading to the onset of the fast growth period for the permeability coefficient. Eventually, as a significant number of foam bubbles dissipate or are flushed from the specimen, the permeation channels tend to be stable, and the growth rate of the permeability coefficient slowed down, making the permeability coefficient of the conditioned sand enters the slow growth period.

The permeability coefficients of foam-conditioned sand with conditioning parameters w=10%/FIR=10% and w =10%/FIR=20% exceeded 10^{-5} m/s when the bottom pressure P_b was 0 and the top pressure P_t was varied to provide different hydraulic gradients, failing to meet the requirement of low permeability (Hu et al. 2020). In this study, the foam-bentonite slurry combined

conditioning (supplemented with bentonite slurry, *BIR*=5%) was employed. As shown in Fig. 4, all conditioned sand specimens maintain an initial permeability coefficient below 10^{-5} m/s for over 90 min. Hence, it is viable to utilize foam and bentonite slurry to prevent water spewing during EPB shield tunnelling in sandy ground under higher hydraulic gradients. In Fig. 4(b)-(d), it is evident that an increase in hydraulic gradient prompts a rapid rise in the permeability coefficient during the fast growth period. With high seepage force, foam bubbles are susceptible to destabilization and flushing out by water flow, disrupting the water-blocking structure. Consequently, permeability channels become fully connected, leading to a swift increase in the permeability coefficient of the conditioned sand. To some extent, the injection of bentonite slurry introduces additional fine particles into the specimens, effectively filling the soil skeleton composed of coarse particles. Simultaneously, the aggregation of these fine bentonite particles enhances the liquid viscosity of the foam and contributes to its stability (Zhao et al. 2016). The combination of fine bentonite particles and foam bubbles reinforces water-blocking structures, resulting in a low permeability coefficient of the conditioned soil over an extended period. Furthermore, fine bentonite particles play a role in stabilizing foam bubbles, as elaborated in Ling et al. (2022).

In Fig. 4(b)-(d), under constant top pressure, increasing the bottom pressure moderately elevates the initial permeability coefficient of conditioned sand. However, this adjustment prolongs the initial stable period and delays the transition to the fast growth period. During the initial stage of permeability tests, foam bubbles and bentonite particles continuously adjust their positions in the soil skeleton under hydrodynamic action to form the most effective water-blocking structures. Augmenting bottom pressure tends to impede this adjustment process. As bottom pressure increases,

the pressure difference between the top and bottom of the sand specimen gradually diminishes, reducing the hydraulic gradient. This, in turn, stabilizes the foam bubbles, making them less prone to dissipation or flushing out. Consequently, foam bubbles effectively become trapped between soil particles, significantly reducing sand permeability and extending the initial stable period of the permeability coefficient. In the fast growth period, liquid drainage and air exchange processes cause foam bubbles to coarsen and dissipate, disrupting the water-blocking structures, leading to a rapid increase in the permeability coefficient. Water flowing through the sand specimen experiences reduced head loss, increased cross-sectional area, and conversion of pressure potential energy into kinetic energy. Interestingly, during the initial stable period, no significant difference in water pressure between the top and bottom gauges is observed due to the stable presence of foam bubbles, as depicted in Fig. 5. Notably, the vertical dotted line in Fig. 5 signifies the time when the permeability coefficient enters the fast growth period, aligning with the time when the pressure difference between the top and bottom of the specimen decreases.

4.2. Effect of water pressure on the migration of fine particles

Figure 6 illustrates the relationship between the permeability coefficient during the slow growth period (k_{sg}) and water pressure. It shows that, with a constant top pressure, k_{sg} decreases as the bottom pressure increases, and the decline rate gradually slows down. Permeability tests reveal that higher water pressures at both the top and bottom of the soil specimen result in a lower permeability coefficient during the slow growth period. This is attributed to the increased stability of foam bubble structures under high pressure, which slows down the rate of foam coarsening compared to lower pressure conditions (Wu et al. 2020). Foam bubbles can effectively sustain their role in lowering

the permeability of sand over an extended duration.

As the hydraulic gradient increases, there is a slight reduction in the permeability coefficient of foam-bentonite slurry-conditioned sand during the slow growth period. This occurs primarily because the elevated seepage force causes fine particles to migrate downward, becoming trapped at the bottom of the permeameter. Consequently, permeability channels are obstructed, and the pores between soil particles are filled, resulting in a decreased permeability coefficient. Another reason for the reduction in k_{sg} is the seepage-induced consolidation process in the conditioned soil with the increase of hydraulic gradient. Fox (1996) noted that soils with high compressibility, such as soft clays and soil-bentonite slurries, are more susceptible to the effects of seepage consolidation than relatively incompressible soils. When the hydraulic gradient increased to a certain extent, the higher effective stress at the bottom of the specimen could lead to the clogging of permeation channels formed by water, as the effective stress was greater at the bottom than at the top. Consequently, with further increases in the hydraulic gradient, the reduction in the permeability coefficient during the slow growth period became weaker and weaker. This phenomenon has also been extensively applied in the context of soil-bentonite backfill for slurry walls (Xu et al. 2016; Zhu et al. 2023).

However, the outlet of the permeameter was connected to the atmosphere in our previous work (Ling et al. 2022). It is still unknown if the effect of water pressure is independently of the hydraulic gradient. In this study, water pressures at the top and bottom of the specimen are both applied. An interesting phenomenon is that even under high hydraulic gradients, the permeability coefficient during the slow growth period remains higher than that under low hydraulic gradients, which also indicates that the hydraulic gradient and water pressure have a coupling effect on the permeability

characteristics of conditioned sand. A detailed analysis focusing solely on the influence of water pressure is presented in Section 4.3.

To further investigate the migration of fine particles under varying water pressures, sand specimens were collected after the permeability tests under four testing conditions (top pressure is 0.161 MPa and bottom pressures are 0.019 MPa, 0.065 MPa, 0.101 MPa and 0.134 MPa, respectively). Specimens were collected from the upper part (20 cm at the top) and the lower part (20 cm at the bottom). After drying and sieving, the grain particle distributions were compared. Figure 7 depicts the results of fine particles migration within three particle size ranges (<0.075 mm, 0.075-0.1 mm, and 0.1-0.25 mm). Observations reveal fine particles migration across all size ranges, with higher content of fine particles at the bottom of the specimen compared to the top (Fig. 7(a)-(d)). For instance, the percentage of particle less than 0.075 mm at the bottom is 1.6 times higher than that at the top (Fig. 7(c)). The proportions of fine particles in both top and bottom sand are higher than before testing due to the addition of bentonite slurry, increasing the fine particles content in the sand specimen. With lower bottom pressure, the difference between the top and the bottom pressure is higher. As a result, the hydraulic gradient increases, the foam structure tends to be unstable, and more fine particles are carried out by water flow. The effect of bentonite slurry on the function of foam for lowering the permeability coefficient of conditioned soil will be weakened. So that the permeability coefficient of the conditioned sand increases faster during the fast growth period and is higher when it reaches the slow growth period, as shown in Fig. 4(d).

4.3. Effect of water pressure on the water-blocking structure of foam bubbles

To investigate the effect of water pressure on the permeability characteristics of conditioned

sand, it is essential to maintain a constant hydraulic gradient, ensuring a consistent seepage force. Figure 8 illustrates the effect of water pressure on the permeability characteristics of sand conditioned with foam and bentonite slurry when the hydraulic gradient remains constant or relatively close. Under constant hydraulic gradients, the time-dependent permeability coefficient curves of the conditioned sand exhibit a slower change rate with increasing top and bottom water pressure. According to Fig. 8(a)-(c), this phenomenon becomes more pronounced with higher hydraulic gradients. In each subfigure, it is evident that the initial stable period of the permeability coefficient shortens or even disappears under lower water pressure. Then, the permeability coefficient passes through the fast growth period and reaches the slow growth period rapidly. For instance, there is no apparent initial stable period observed when P_t=0.096 MPa/P_b=0 MPa/i=18.2 (see pink dotted line in Fig. 8(c)).

Figure 9 shows the existence state of the foam bubbles in the sand specimen during permeability tests observed from the permeameter wall. In the test conditions of P_t=0.096 MPa / P_b=0 MPa / i=18.2 (low water pressure) and P_t=0.161 MPa / P_b=0.065 MPa / i=18.2 (high water pressure), it is evident that foam bubbles coarsen and dissipate quickly under low water pressure. In Fig. 9(a), at the beginning of the permeability test (t=1 min), numerous foam bubbles of varying sizes occupy the pores. However, by t=224 min, many small bubbles become imperceptible due to foam bubble instability. At t=813 min, the majority of foam bubbles have dissipated. In Fig. 9(b), at t=1 min, a large number of foam bubbles accumulate in the soil pores. Over time, from t=1514 min to t=2417 min, there is minimal change in foam size and quantity. Notably, the foam degradation process proceeds at a slower pace under high water pressure, ensuring that foam bubbles maintain a smaller

size for an extended period. This phenomenon aligns with the findings of Wu et al. (2018) regarding foam size under different pressure conditions, and it can be attributed to the foam degradation mechanisms mentioned in the Section 2. The internal pressures of bubbles with small sizes are almost same, so that the bubbles are more stable because there is less air exchange occurring between them. Another plausible explanation lies in the fact that it takes more time for liquid to drain from smaller bubbles compared to larger bubbles. This is due to the increased surface area of smaller bubbles, leading to a longer drainage path for liquids. Therefore, the stability of the water-blocking structure is significantly enhanced, resulting in that the permeability coefficient of conditioned soil change more gradually under high water pressure.

5. Discussion

5.1. Analysis of the stability of foam structure under water pressure

The foam commonly employed in soil conditioning for shield tunnelling is typically considered dry foam with $FER \geq 10$ and an air content of 90% or higher (Huang et al. 2007; Wang et al. 2021b). As mentioned in Section 2, foam dissipation primarily involves two mechanisms: liquid film drainage and air exchange. In the case of dry foam, the liquid content in foam is low, and air exchange becomes a dominant dissipation mode. Figure 10 illustrates the state of foam bubbles before and after the introduction of high water pressure (P_w) into the pores of the soil skeleton.

According to the Young-Laplace equation shown in Eq. (1), the relation between the internal and external pressure difference of foam bubbles and bubble radius can be obtained as follows:

$$P_1 - P_2 = \frac{2\sigma_1}{R_1} \tag{1}$$

where P_1 and P_2 are the internal and external pressures of the bubble before introducing water pressure, respectively; σ_1 represents surface tension before introducing water pressure; R_1 denotes bubble radius before introducing water pressure.

The air in the foam conforms to the general gas equation, as shown in Eq. (2). In addition, the air in the foam bubbles before and after introducing water pressure conforms to Boyle's law, as shown:

$$PV = nRT \tag{2}$$

$$P_1V_1 = P_1'V_1' \tag{3}$$

where P_1 and P_1' are the internal pressure of the bubble before and after introducing water pressure, respectively; V_1 and V_1' denote the volume of the bubble before and after introducing water pressure, respectively.

Combining Eqs. (1) and (3) yields

$$\frac{P_1}{P_1'} = \frac{V_1'}{V_1} = \left(\frac{R_1'}{R_1}\right)^3 = \frac{\frac{2\sigma_1}{R_1} + P_2}{\frac{2\sigma_1'}{R_1'} + P_2'} \tag{4}$$

where P_2' is the external pressure of the bubble after introducing water pressure ($P_2'=P_2+P_w$); σ_1' and R_1' are surface tension and bubble radius after introducing water pressure, respectively.

After increasing water pressure, $P_2'>P_2$ and the increase in surface tension (σ_1') is negligible compared to the increase in external pressure (P_2'). Therefore, it can be reasonably disregarded. In summary, the value of Eq. (4) is less than 1, indicating that the bubble radius under high water

pressure (R_1') is smaller than that under low water pressure (R_1). The reduced bubble radius results in a more stable foam structure, enhancing the stability of the bubbles themselves. This stability reduces the coarsening of adjacent bubbles through air exchange and leads to more stable water-blocking structures within the soil pores. The test results presented in Fig. 9 also support the positive effect of the mentioned water pressure on foam stability.

5.2. Risk analysis of EPB shield standstill and restart based on chamber pressure dissipation

The conditioned soil fills the excavation chamber and screw conveyor, creating an impermeable barrier to balance earth pressure and water pressure ahead of the excavation face. However, during EPB shield tunnelling, temporary halts for equipment maintenance or muck transportation delays are common. With prolonged downtime, foam bubbles dissipation within the conditioned soil occurs in both the excavation chamber and screw conveyor, leading to pressure dissipation (Bezuijen and Dias 2017). As downtime extends, the pressure in the chamber may no longer counterbalance the pressure ahead of the excavation face, potentially compromising the water-blocking structure. This can create new permeability channels, increasing the risk of water spewing upon shield restart. In the case of a long-time standstill, the conditioning state of the muck in the excavation chamber and screw conveyor was shown in Fig. 11. The pressure at the top of the excavation chamber was lower than that at the bottom, and similarly, the pressure at the outlet of the screw conveyor was lower than that at the inlet, causing faster foam degradation rate at the top of the excavation chamber and the outlet of the screw conveyor. Consequently, foam bubbles in these areas grow larger and are more prone to dissipation.

In addition, the total stress and pore pressure of the conditioned soil in the screw conveyor decrease linearly from the inlet to the outlet (Bezuijen and Schaminée 2001; Merritt and Mair 2006). Hence, foam bubbles near the outlet of the screw conveyor are more prone to coarsening and dissipating. Permeability distribution within the conditioned soil in the screw conveyor is non-uniform and varies along the direction of muck transport. As shown in Fig. 11, the height between the groundwater level and the bottom of the shield is H, and the height between any point in the screw conveyor and the bottom of the shield is h_i (the corresponding heights of A, B and C in the figure are h_1, h_2 and h_3, respectively). The water pressure decreases gradually along the direction of transporting muck and dropped to 0 at the outlet of the screw conveyor (point C). Combined with the test results in Fig. 8, it is evident that foam stability decreases as water pressure decreases. So, the permeability coefficient of the conditioned soil increases rapidly over time, potentially peaking at the screw conveyor outlet. It is recommended to use the permeability coefficient determined under the minimum water pressure as the evaluation index for assessing the risk of water spewing.

In summary, the decreasing pressure in the screw conveyor leads to higher permeability in the conditioned soil at the screw conveyor outlet. To ensure the safety of shield tunnelling, it is crucial to validate that the permeability coefficient of the conditioned soil at the screw conveyor outlet meets the permeability requirements (lower than 10^{-5} m/s and maintain at least 90 min). Based on the test results, foam-bentonite slurry-conditioned sand can meet the permeability requirements even under high water pressure. Therefore, the combined conditioning with foam and bentonite slurry proves effective in maintaining pressure stability in the excavation chamber and screw conveyor when the shield restarts after extended downtime due to equipment maintenance, cutter

changes, or emergencies.

6. Conclusion

This study investigated the effect of water pressure on the time-dependent permeability characteristics of sand conditioned with foam and bentonite slurry by conducting permeability tests at varying top and bottom water pressures. The novel contributions of this work are as follows:

(1) Combining foam with bentonite slurry significantly outperforms the use of foam alone for sand conditioning. Sand conditioned with foam and bentonite slurry achieved a permeability coefficient of less than 10^{-5} m/s, sustained for over 90 min. Furthermore, increasing water pressure at both the top and bottom extended the initial stable period of the permeability coefficient in conditioned sand, reduced the growth rate during the fast growth period, and delayed the transition to the slow growth period.

(2) Fine particles migration from top to bottom elevated the concentration of fine particles at the base of the sand specimen, especially pronounced under increasing water pressure, resulting in a reduction of the permeability coefficient during the slow growth period. With constant top pressure, the permeability coefficient decreased as the bottom pressure increased during this period. This decline was primarily due to the diminishing seepage force caused by a declining hydraulic gradient, coupled with reduced ease of foam bubble dissipation.

(3) Under a constant hydraulic gradient, increasing both top and bottom pressure resulted in a reduction of the permeability coefficient in the conditioned sand. As water pressure increased, foam bubbles exhibited improved stability, maintaining a smaller size, and reducing the rate of foam

coarsening. Enhanced foam bubble stability contributed to a more effective reduction in the permeability coefficient of the conditioned sand.

(4) The test results indicate that when the water outlet is connected to the air, the calculated permeability coefficient is the largest, representing the most conservative approach from an engineering safety perspective. It is recommended to use the permeability coefficient of conditioned soil at the outlet of the screw conveyor with the lowest water pressure as an indicator to assess the risk of water spewing when carrying out permeability tests.

It is important to note that while the test results serve as a valuable indicator, they may not fully reflect field behaviour due to the inherent scale limitations of laboratory-tested sand specimens. Increasing the specimen length can introduce various seepage patterns and fine particles migration, potentially altering the conditioning state of the sand. Additional field tests will be conducted in the next step to validate the suitability of the proposed evaluation indicator in permeability tests for shield engineering applications. Furthermore, it's crucial to acknowledge that the calculation of the permeability coefficient of the conditioned soil using Darcy's law still relies on certain assumptions, such as the homogeneity of the specimen over short measurement intervals. This highlights the necessity of employing specialized equipment and procedures to accurately determine permeability coefficients, providing precise insights into the permeability characteristics of conditioned soil.

Acknowledgements

The financial support from National Natural Science Foundation of China (No. 52022112) is acknowledged and appreciated. The authors are also grateful for the comments provided by the editors and four anonymous reviewers.

Competing interests statement

The authors declare there are no competing interests.

Data availability statement

Data generated or analysed during this study are available from the corresponding author upon reasonable request.

Reference

API (American Petroleum Institute) (2003). Recommended practice standard procedure for field testing water-based drilling fluids, 13B-1, 3rd ed. Washington, DC, USA: American Petroleum Institute.

ASTM (American Society for Testing and Materials) (2017). Standard Practice for Classification of Soils for Engineering Purposes (Unified Soil Classification System): ASTM D2487-17. ASTM International, West Conshohocken, PA.

ASTM (American Society for Testing and Materials) (2019). Standard test method for permeability of granular soils (constant head): ASTM D2434-19. ASTM International, West Conshohocken, PA.

Bezuijen, A., Schaminée, P., and Kleinjan, J. (1999). Additive testing for earth pressure balance shields. In Proceedings Twelfth European Conference on Soil Mechanics and Geotechnical Engineering, pp. 1991-1996. Amsterdam, Netherlands.

Bezuijen, A., and Schaminée, P. (2001). Simulation of the EPB-shield TBM in model tests with foam as additive. In Modern tunnelling science and technology, Kyoto, pp. 935-940. Rotterdam: Balkema.

Bezuijen, A., and Dias, T. (2017). EPB, chamber pressure dissipation during standstill. EURO: TUN 2017 - 4th International Conference on Computational Methods in Tunnelling and Subsurface Engineering, 1, 225-231. Innsbruck, Austria.

Borio, L., and Peila, D. (2010). Study of the permeability of foam conditioned soils with laboratory tests. American Journal of Environmental Sciences. 6(4): 365-370.

Budach, C. (2012). Untersuchungen zum erweiterten Einsatz von Erddruckschilden in

grobkörnigem Lockergestein (Transl.: Investigations for extended use of EPB Shields in coarse-grained soils). PhD. thesis. Ruhr-Universität Bochum.

Budach, C., and Thewes, M. (2015). Application ranges of EPB shields in coarse ground based on laboratory research. Tunnelling and Underground Space Technology. 50: 296-304.

Chapuis, R. (1990). Sand-bentonite liners: predicting permeability from laboratory tests. Canadian Geotechnical Journal. 27(1): 47-57.

Chen, Z., Bezuijen, A., Fang, Y., et al. (2022). Experimental study and field validation on soil clogging of EPB shields in completely decomposed granite. Tunnelling and Underground Space Technology. 120: 104300.

EFNARC. (2005). Specification and guidelines for the use of specialist products for mechanised tunnelling (TBM) in soft ground and hard rock.

Feng, Z., Wang, S., Qu, T., et al. (2023). Experimental study on workability and permeability of sandy soils conditioned with thickened foam. Journal of Rock Mechanics and Geotechnical Engineering. In Press, Journal Pre-proof. https://doi.org/10.1016/j.jrmge.2023.05.015.

Fox, P. (1996). Analysis of hydraulic gradient effects for laboratory hydraulic conductivity testing. Geotechnical Testing Journal, 19(2): 181-190.

Hu, Q., Wang, S., Qu, T., et al. (2020). Effect of hydraulic gradient on the permeability characteristics of foam-conditioned sand for mechanized tunnelling. Tunnelling and Underground Space Technology. 99: 103377.

Huang, J., and Sun, Q. (2007). Advances in the mechanism of liquid foam percolation. Advances in Mechanics. 37(2): 269-278 (in Chinese).

Huang, S., Wang, S., Xu, C., et al. (2019). Effect of grain gradation on the permeability

characteristics of coarse-grained soil conditioned with foam for EPB shield tunneling. KSCE Journal of Civil Engineering. 23(11): 4662-4674.

Jancsecz, S., Krause, R., and Langmaack, L. (1999). Advantages of soil conditioning in shield tunnelling: experiences of LRTS Izmir. Proc., Int. Congr. Challenges for the 21st Century, Balkema Rotterdam, pp. 865-875.

Kaptay, G. (2006). On the equation of the maximum capillary pressure induced by solid particles to stabilize emulsions and foams and on the emulsion stability diagrams. Colloids and Surfaces A Physicochemical and Engineering Aspects. 282: 387-401.

Kenney, T., Veen, W., Swallow, M., et al. (1992). Hydraulic conductivity of compacted bentonite-sand mixtures. Canadian Geotechnical Journal. 29(3): 364-374.

Komine, H. (2010). Predicting hydraulic conductivity of sand–bentonite mixture backfill before and after swelling deformation for underground disposal of radioactive wastes. Engineering Geology. 114(3): 123-134.

Langmaack, L., and Lee, K. (2016). Difficult ground conditions? Use the right chemicals! Chances–limits–requirements. Tunnelling and Underground Space Technology. 57: 112-121.

Ling, F., Wang, S., Hu, Q., et al. (2022). Effect of bentonite slurry on the function of foam for changing the permeability characteristics of sand under high hydraulic gradients. Canadian Geotechnical Journal. 59(7): 1061-1070.

Ling, F., Wang, S., Zheng, X., et al. (2024). A Novel Calculation Model for the Permeability Coefficient of Soils Conditioned with Foam and Bentonite Slurry. KSCE Journal of Civil Engineering. https://doi.org/10.1007/s12205-024-2017-0.

Ma, G., He, X., Jiang, X., et al. (2021). Strength and permeability of bentonite-assisted biocemented

coarse sand. Canadian Geotechnical Journal. 58(7): 969-981.

Merritt, A., and Mair, R. (2006). Mechanics of tunnelling machine screw conveyors: model tests. Géotechnique. 56(9): 605-615.

Milligan, G. (2000). Lubrication and soil conditioning in tunnelling, pipe jacking and micro-tunnelling: a state-of-the-art review. Geotechnical Consulting Group, London, UK.

Mori, L., Alavi, E., and Mooney, M. (2017). Apparent density evaluation methods to assess the effectiveness of soil conditioning. Tunnelling and Underground Space Technology. 67(8): 175-186.

Peila, D., Oggeri, C., and Vinai, R. (2007). Screw Conveyor Device for Laboratory Tests on Conditioned Soil for EPB Tunneling Operations. Journal of Geotechnical and Geoenvironmental Engineering. 133(12): 1622-1625.

Peila, D., Borio, L., and Pelizza, S. (2011). The behaviour of a two-component backfilling grout used in a tunnel-boring machine. Acta Geotechnica Slovenica. 8(1): 5-15.

Peila, D. (2014). Soil conditioning for EPB shield tunnelling. KSCE Journal of Civil Engineering. 18(3): 831-836.

Peila, D., Picchio, A., Martinelli, D., et al. (2016). Laboratory tests on soil conditioning of clayey soil. Acta Geotechnica. 11: 1061-1074.

Pitois, O., Lorenceau, E., Louvet, N., et al. (2009). Specific surface area model for foam permeability. Langmuir the Acs Journal of Surfaces and Colloids, 25(1): 97-100.

Psomas, S. (2001). Properties of foam/sand mixtures for tunnelling applications. Master's degree thesis, University of Oxford, Oxford, UK.

Quebaud, S., Sibai, M., and Henry, J. (1998). Use of chemical foam for improvements in drilling

by earth-pressure balanced shields in granular soils. Tunnelling and Underground Space Technology. 13(2): 173-180.

Rangel, J., Aguilar, M., Comulada-Simpson, M., et al. (2012). Mexico City deep eastern drainage tunnel. Geotechnical Aspects of Underground Construction in Soft Ground. Geotechnical Aspects of Underground Construction in Soft Ground.

Sivapullaiah, P., Sridharan, A., and Stalin, V. (2000). Hydraulic conductivity of bentonite-sand mixtures. Canadian Geotechnical Journal. 37(2): 406-413.

Vinai, R., Oggeri, C., and Peila, D. (2008). Soil conditioning of sand for EPB applications: a laboratory research. Tunnelling and Underground Space Technology. 23(3): 308-317.

Wang, S., Hu Q., Wang H., et al. (2020a). Permeability characteristics of poorly graded sand conditioned with foam in different conditioning states. Journal of Testing and Evaluation. 49. https://doi.org/10.1520/JTE20190539.

Wang, S., Huang, S., Qiu, T., et al. (2020b). Analytical study of the permeability of a foam-conditioned soil. International Journal of Geomechanics. 20(8): 06020019.

Wang, H., Wang, S., Zhong, J., et al. (2021a). Undrained compressibility characteristics and pore pressure calculation model of foam-conditioned sand. Tunnelling and Underground Space Technology. 118: 104161.

Wang, S., Huang, S., Zhong, J., et al. (2021b). Permeability stability calculation model of foam-conditioned soil based on the permeability constant. International Journal for Numerical and Analytical Methods in Geomechanics. 45(4): 540-559.

Wang, S., Liu, P., Gong, Z., et al. (2022). Auxiliary air pressure balance mode for EPB shield tunneling in water-rich gravelly sand strata: Feasibility and soil conditioning. Case Studies in

Construction Materials. 16: e00799.

Wei, Y., Yang, Y., Tao, M., et al. (2020). Earth pressure balance shield tunneling in sandy gravel deposits: a case study of application of soil conditioning. Bulletin of Engineering Geology and the Environment. 79: 5013-5030.

Wilms, J. (1995). Influence of properties of the support medium on the wear of EPB-shields. MSc Thesis, University of Duisburg-Essen, Duisburg, Germany.

Wu, Y., Mooney, M., and Cha, M. (2018). An experimental examination of foam stability under pressure for EPB TBM tunneling. Tunnelling and Underground Space Technology. 77: 80-93.

Wu, Y., Nazem, A., Meng, F., et al. (2020). Experimental study on the stability of foam-conditioned sand under pressure in the EPBM chamber. Tunnelling and Underground Space Technology. 106: 103590.

Xie, Y., Li, J., Lu, Z., et al. (2018). Effects of bentonite slurry on air-void structure and properties of foamed concrete. Construction and Building Materials. 179(10): 207-219.

Xu, H., Zhu, W., Qian, X., et al. (2016). Studies on hydraulic conductivity and compressibility of backfills for soil-bentonite cutoff walls. Applied Clay Science, 132: 326-335.

Xu, T., and Bezuijen, A. (2018). Bentonite slurry infiltration into sand: filter cake formation under various conditions. Géotechnique. 69(12): 1095-1106.

Xu, T., and Bezuijen, A. (2019). Experimental study on the mechanisms of bentonite slurry penetration in front of a slurry TBM. Tunnelling and Underground Space Technology. 93(11): 103052.

Zhao, G., Dai, C., Wen, D., et al. (2016). Stability mechanism of a novel three-phase foam by adding dispersed particle gel. Colloids and Surfaces A: Physicochemical and Engineering Aspects.

497: 214-224.

Zhu, K., Zhang, K., and He, Y. (2023). Hydro-mechanical behavior and microstructure evolution of red clay-bentonite backfills. Applied Clay Science, 244: 107111.

List of figures:

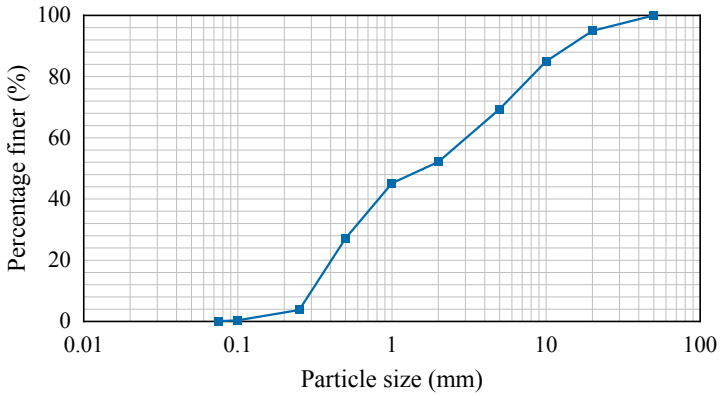

Fig. 1. Grain size distribution of the test sand.

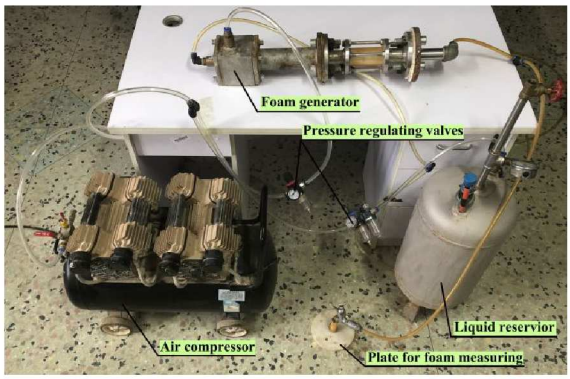

(a)

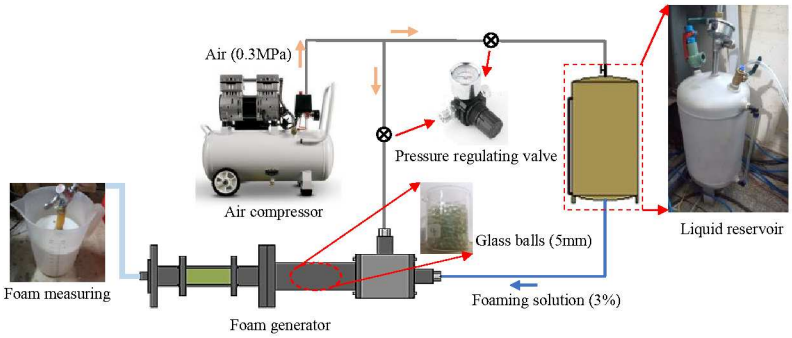

(b)

Fig. 2. Foaming generating system: (a) Picture of the foaming generating system; (b) Schematic diagram of the foaming generating system.

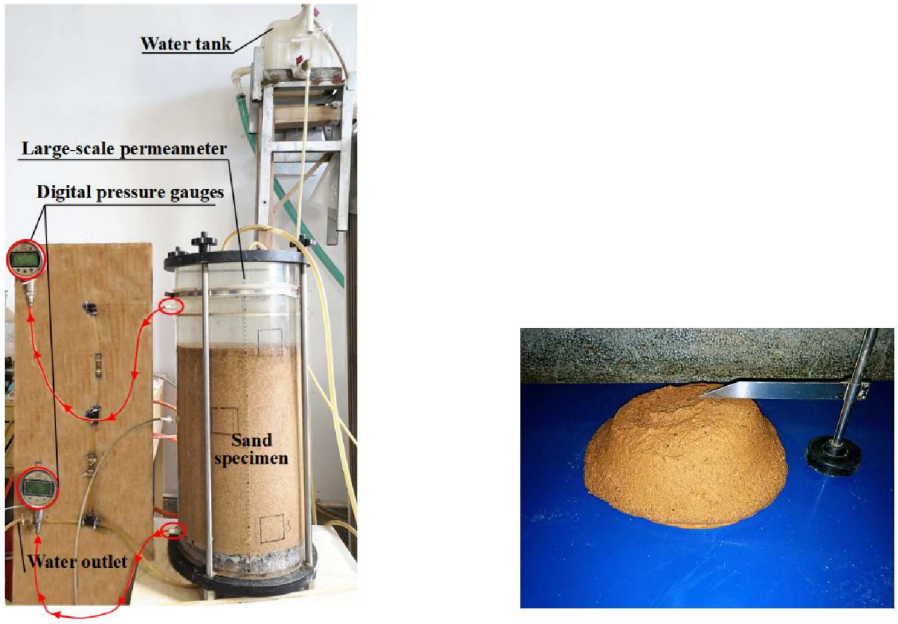

(a) (b)

Fig. 3. Experimental equipment and sand specimen: (a) permeameter; (b) Sand conditioned with foam and bentonite slurry (w=10%, FIR=10% and BIR=5%).

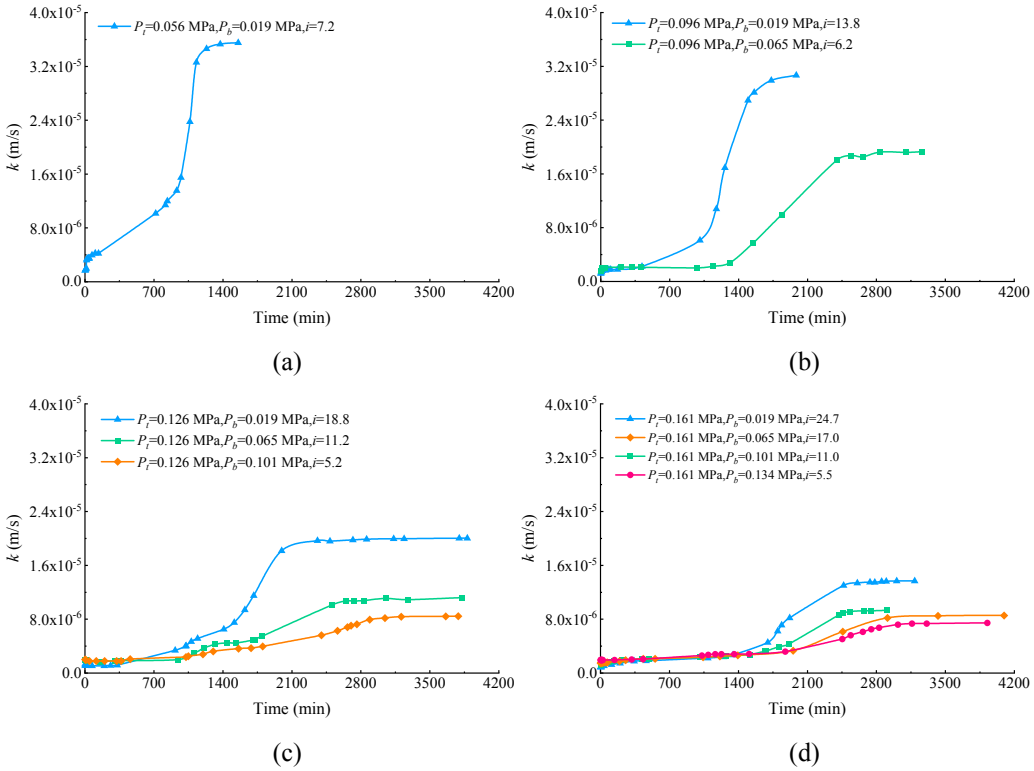

Fig. 4. Time-dependent curves of permeability coefficient under different water pressure: (a) P_t=0.056 MPa; (b) P_t=0.096 MPa; (c) P_t=0.126 MPa; (d) P_t=0.161 MPa.

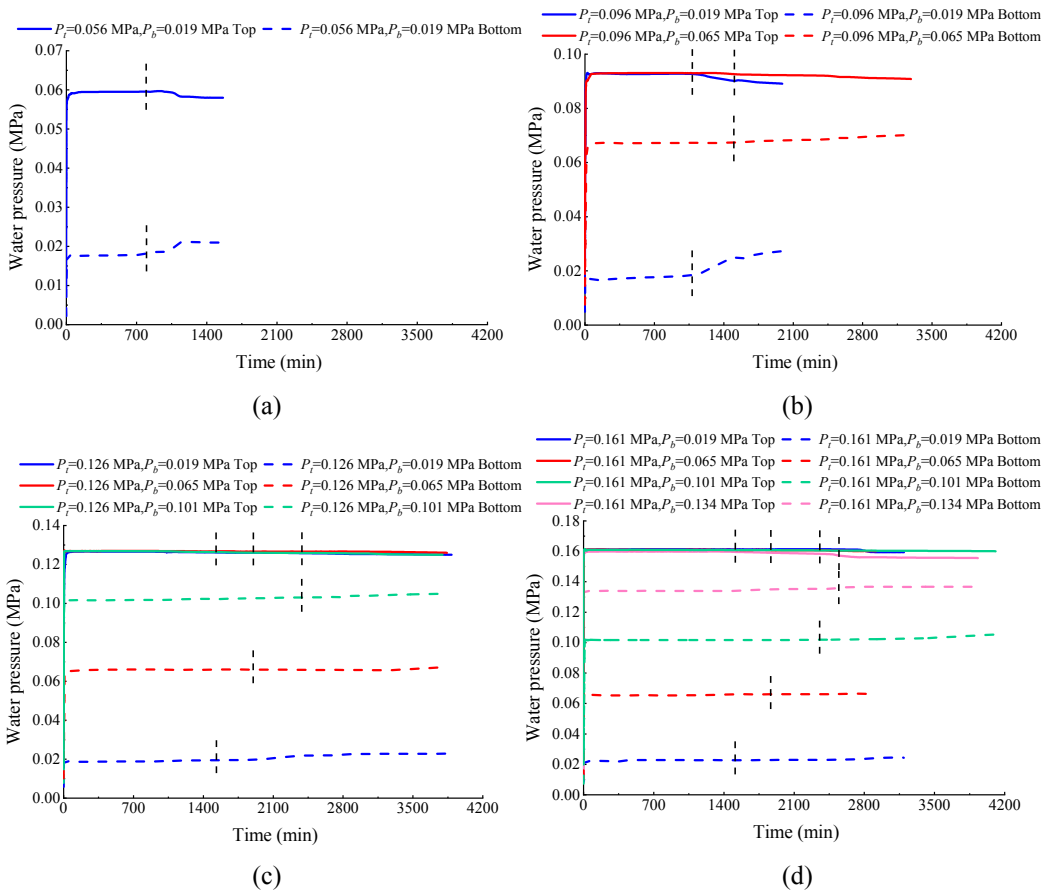

Fig. 5. Time-dependent curves of water pressure for permeability tests: (a) P_t=0.056 MPa; (b) P_t=0.096 MPa; (c) P_t=0.126 MPa; (d) P_t=0.161 MPa.

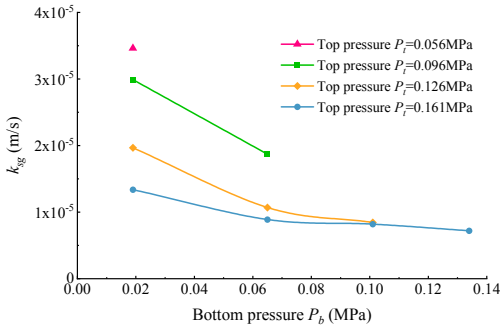

Fig. 6. Effect of the water pressure on the permeability coefficient in the slow growth period.

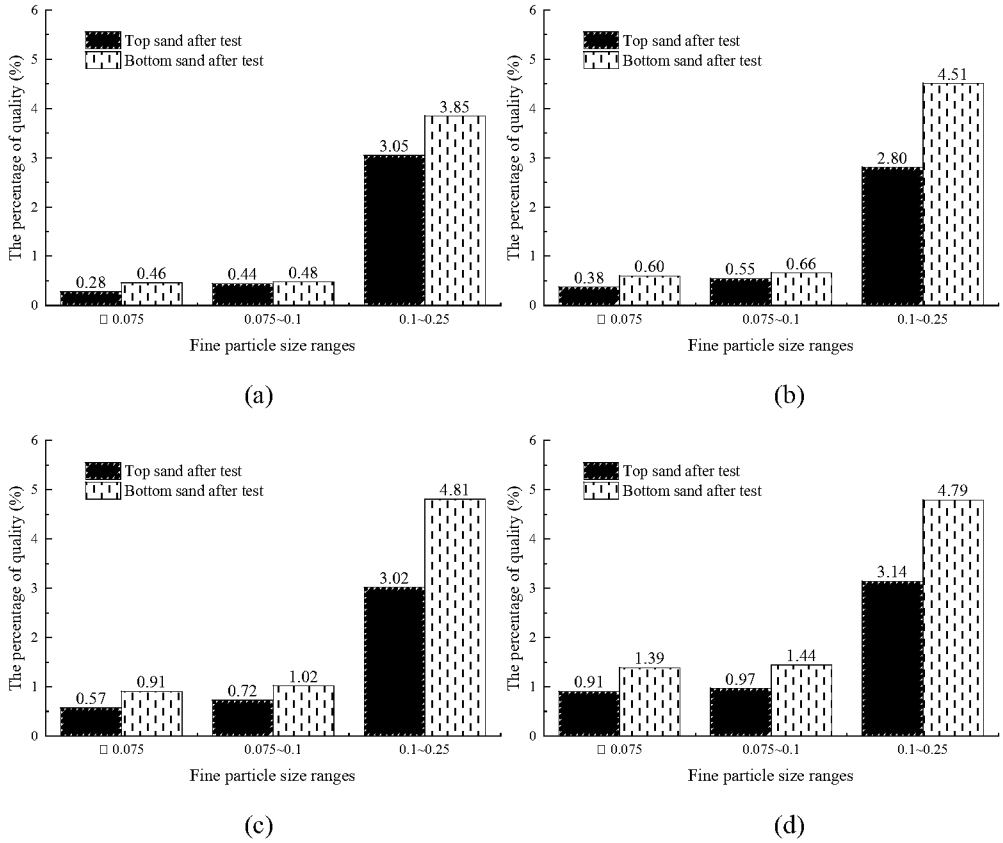

Fig. 7. The mass percentage of fine particles under constant top pressure (P_t=0.161 MPa) and different bottom water pressures: (a) P_b=0.019 MPa; (b) P_b=0.065 MPa; (c) P_b=0.101 MPa; (d) P_b=0.134 MPa.

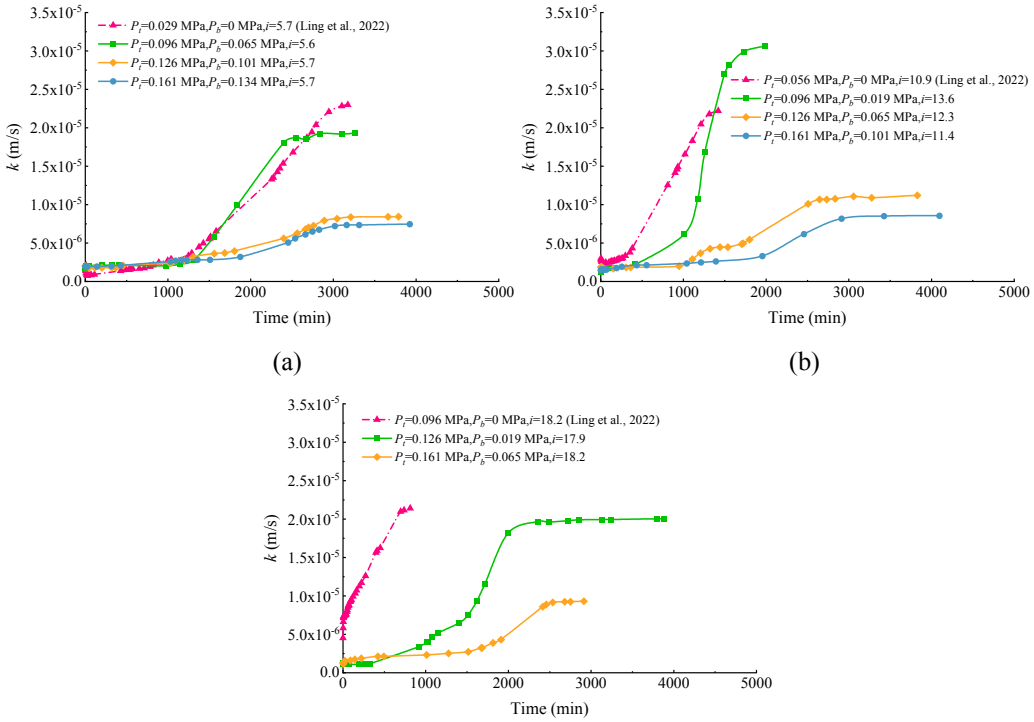

Fig. 8. Effect of water pressure on permeability coefficient under different hydraulic gradients: (a) i≈5.7; (b) i≈12.0; (c) i≈18.0.

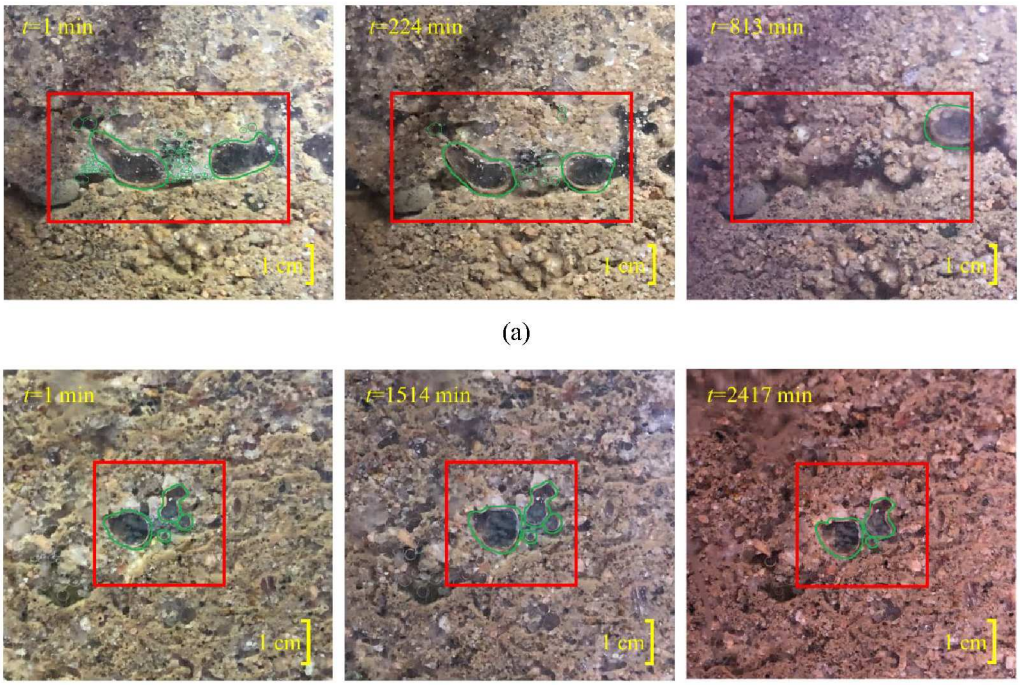

Fig. 9. The existence state of the foam bubbles during the permeability tests: (a) under low water pressure (P_t=0.096 MPa/P_b=0 MPa/i=18.2); (b) under high water pressure (P_t=0.161 MPa/P_b=0.065 MPa/i=18.2).

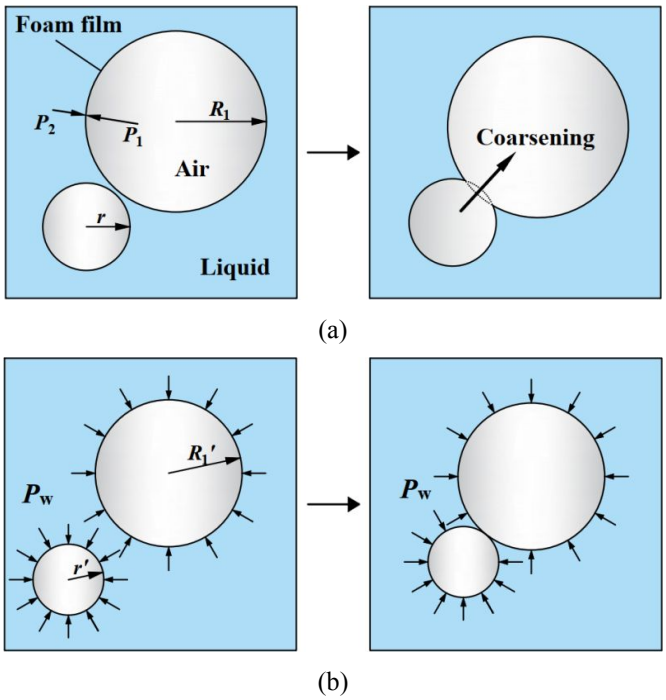

Fig. 10. The existence of foam bubbles: (a) no water pressure; (b) under water pressure.

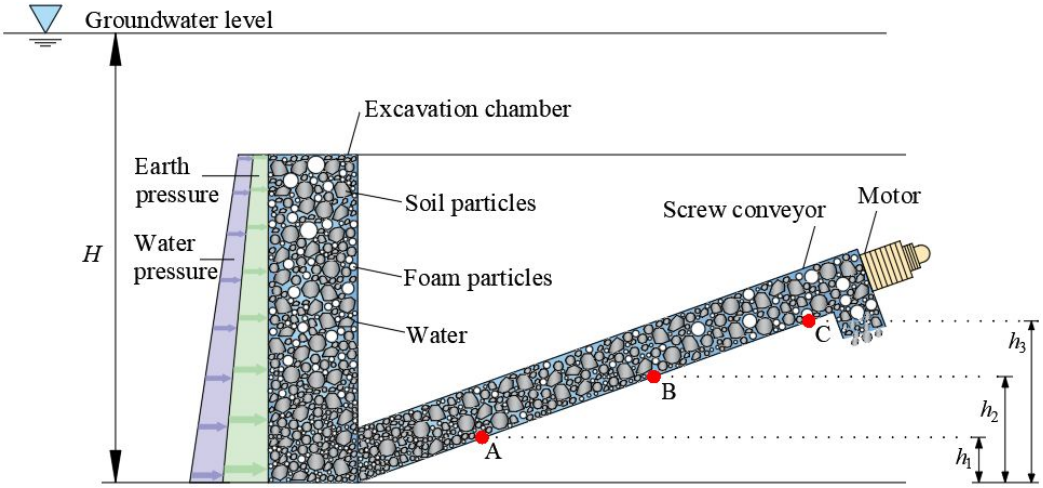

Fig. 11. Schematic diagram of EPB shield standstill below groundwater level in full chamber mode.

List of tables

Table 1 Chemical compositions of the foam agent.

Name	Percent	Function
Sodium dodecyl sulphate	1~1.5%	Anionic surfactant
Dodecyl ammonium chloride	3~3.5%	Cationic surfactant
Silicone oil	1~2%	Foam stabilizer
Water	93~94%	Solvent

Table 2 Mineral composition of the sodium bentonite.

Mineral name	Chemical formula	Weight percentage (%)
Na-montmorillonite	$Na_{0.3}(Al,Mg)_2Si_4O_{10}(OH)_2$	48.8
Ca-montmorillonite	$Ca_{0.2}(Al,Mg)_2Si_4O_{10}(OH)_2$	14.1
Soda feldspar	$NaAlSi_3O_8$	28.3
Microcline	$(K_{0.95}Na_{0.05})$ $(AlSi_3O_8)$	5.5
Quartz	SiO_2	2.5
Calcite	$CaCO_3$	0.8

Table 3 Testing conditions of the permeability tests.

Water content, w	Foam injection ratio, *FIR*	Bentonite slurry injection ratio, *BIR*	Conditioning state	Top pressure, P_t (MPa)	Bottom pressure, P_b (MPa)	Initial hydraulic gradients, i
10%	10%	5%	Suitable conditioning	0.056	0.019	7.2
				0.096	0.019	13.8
				0.096	0.065	6.2
				0.126	0.019	18.8
				0.126	0.065	11.2
				0.126	0.101	5.2
				0.161	0.019	24.7
				0.161	0.065	17.0
				0.161	0.101	11.0
				0.161	0.134	5.5